View metadata, citation and similar papers at core.ac.uk

brought to you by CORE

provided by Acronym

Citation: CPT Pharmacometrics Syst. Pharmacol. (2019) 8, 296–307; doi:10.1002/psp4.12397

ARTICLE

# Physiologically-Based Pharmacokinetic Models for CYP1A2 Drug–Drug Interaction Prediction: A Modeling Network of Fluvoxamine, Theophylline, Caffeine, Rifampicin, and Midazolam

Hannah Britz[1], Nina Hanke[1], Anke-Katrin Volz[1], Olav Spigset[2,3], Matthias Schwab[4,5,6], Thomas Eissing[7], Thomas Wendl[7], Sebastian Frechen[7] and Thorsten Lehr[1,*]

**This study provides whole-body physiologically-based pharmacokinetic models of the strong index cytochrome P450 (CYP)1A2 inhibitor and moderate CYP3A4 inhibitor fluvoxamine and of the sensitive CYP1A2 substrate theophylline. Both models were built and thoroughly evaluated for their application in drug–drug interaction (DDI) prediction in a network of perpetrator and victim drugs, combining them with previously developed models of caffeine (sensitive index CYP1A2 substrate), rifampicin (moderate CYP1A2 inducer), and midazolam (sensitive index CYP3A4 substrate). Simulation of all reported clinical DDI studies for combinations of these five drugs shows that the presented models reliably predict the observed drug concentrations, resulting in seven of eight of the predicted DDI area under the plasma curve (AUC) ratios (AUC during DDI/AUC control) and seven of seven of the predicted DDI peak plasma concentration ($C_{max}$) ratios ($C_{max}$ during DDI/$C_{max}$ control) within twofold of the observed values. Therefore, the models are considered qualified for DDI prediction. All models are comprehensively documented and publicly available, as tools to support the drug development and clinical research community.**

## Study Highlights

**WHAT IS THE CURRENT KNOWLEDGE ON THE TOPIC?**

☑ Physiologically-based pharmacokinetic (PBPK) models are a valuable tool to investigate and predict the drug–drug interaction (DDI) potential of investigational drugs. A publicly available library of thoroughly and transparently evaluated models of relevant perpetrator and victim drugs used in clinical studies is needed to accelerate the drug development process.

**WHAT QUESTION DID THIS STUDY ADDRESS?**

☑ The aim of this study was to provide whole-body PBPK models of the most important cytochrome (CYP)1A2 perpetrator and victim drugs and to evaluate them for their application in PBPK DDI modeling.

**WHAT DOES THIS STUDY ADD TO OUR KNOWLEDGE?**

☑ This study provides publicly available and transparently built and evaluated PBPK models of fluvoxamine and theophylline. Both models integrate the current knowledge on relevant pharmacokinetic (PK) mechanisms, including the impact of different genotypes and smoking on the PK of fluvoxamine.

**HOW MIGHT THIS CHANGE DRUG DISCOVERY, DEVELOPMENT, AND/OR THERAPEUTICS?**

☑ The developed PBPK models are ready to use for their application in DDI modeling and might help to support the drug development process.

Cytochrome P450 (CYP)1A2 is an important enzyme for the metabolism of several endogenous substances (e.g., melatonin), and it is involved in the elimination of 15% of all therapeutic drugs.[1] CYP1A2 is exclusively expressed in the liver, where it accounts for about 13% of total CYP content in liver microsomes.[2] The expression of CYP1A2 can be markedly induced by smoking, whereas rifampicin, a strong CYP3A4 inducer, shows only a moderate potential to induce CYP1A2.[1,3] Well-known substrates of CYP1A2 include caffeine and theophylline, which are mainly metabolized via CYP1A2 (fractions metabolized of 0.95[4] and 0.7,[5,6] respectively) and can, therefore, be used as sensitive CYP1A2 substrates to evaluate the activity of CYP1A2 *in vivo*.[7] The most important inhibitor of CYP1A2 is fluvoxamine.

[1]Clinical Pharmacy, Saarland University, Saarbrücken, Germany; [2]Department of Clinical and Molecular Medicine, Norwegian University of Science and Technology, Trondheim, Norway; [3]Department of Clinical Pharmacology, St. Olav University Hospital, Trondheim, Norway; [4]Dr. Margarete Fischer-Bosch-Institute of Clinical Pharmacology, Stuttgart, Germany; [5]Department of Clinical Pharmacology, University Hospital Tübingen, Tübingen, Germany; [6]Department of Pharmacy and Biochemistry, University Tübingen, Tübingen, Germany; [7]Clinical Pharmacometrics, Bayer AG, Leverkusen, Germany. *Correspondence: Thorsten Lehr (thorsten.lehr@mx.uni-saarland.de)

Received: November 8, 2018; accepted: January 30, 2019. doi:10.1002/psp4.12397

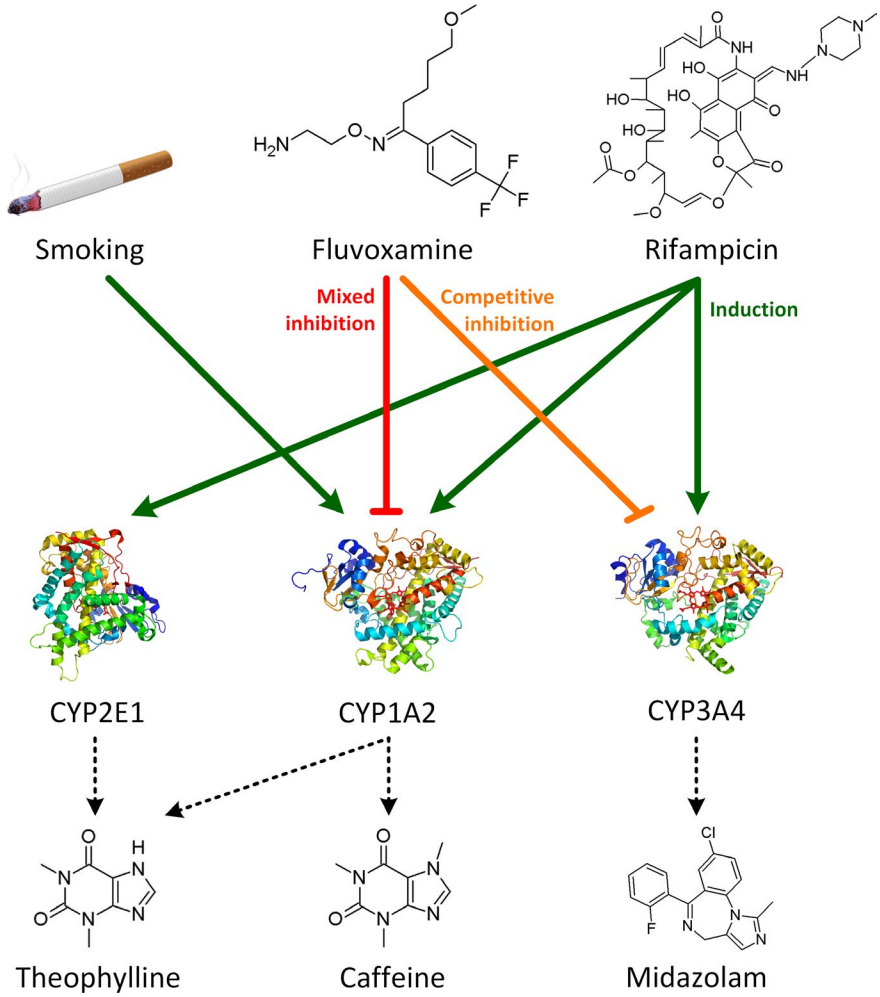


**Figure 1** Cytochrome P450 (CYP) 1A2 drug–drug interaction (DDI) network. Schematic illustration of the developed CYP1A2 DDI network with fluvoxamine and rifampicin as CYP1A2 perpetrator drugs and theophylline and caffeine as CYP1A2 victim drugs. Midazolam was used as CYP3A4 victim drug for fluvoxamine. Dark green lines indicate induction by rifampicin or smoking, and the red and orange lines indicate inhibition by fluvoxamine.

The US Food and Drug Administration (FDA) specifies caffeine as a sensitive clinical index substrate and fluvoxamine as a strong clinical index inhibitor for CYP1A2. Furthermore, they recommend considering a clinical study in smokers for investigational drugs that are CYP1A2 substrates.[8] Theophylline is classified as a sensitive clinical substrate and rifampicin as moderate clinical inducer of CYP1A2.[9]

Physiologically-based pharmacokinetic (PBPK) modeling is a valuable method, recognized by the FDA and the European Medicines Agency, to explore and quantitatively predict the pharmacokinetics (PK) of drugs, to evaluate drug–drug interactions (DDIs), and to support clinical study design, dose selection, and labeling.[8,10–12] The FDA furthermore supports the prediction of DDI studies with weak and moderate index inhibitors and inducers as an alternative to prospective clinical studies, if the sponsors can demonstrate adequate model performance using clinical data from DDI studies with strong index perpetrators.[8]

The aim of this study was to develop a PBPK DDI network for CYP1A2 and thereby to extend the library of publicly available PBPK models for DDI prediction.[13,14] For this purpose, whole-body PBPK models of fluvoxamine and theophylline have been developed and existing models of

**Figure 2** Fluvoxamine plasma concentrations. (**a**) Population predictions of selected fluvoxamine plasma concentration-time profiles compared with observed data in linear (left panel) and semilogarithmic plots (right panel). The upper panel shows i.v. application, the lower panel p.o. administration of fluvoxamine. Observed data are shown as dots ± SD.[34,35] Population simulation arithmetic means are shown as lines; the shaded areas illustrate the 68% population prediction intervals. (**b**) Predicted compared with observed fluvoxamine plasma concentration values of all clinical studies. Line of identity and 0.5-fold to 2.0-fold acceptance limits are shown as black lines. The 0.8-fold to 1.25-fold limits are shown as grey lines. Details on dosing regimens and study populations are listed in **Table S1a of Supplement S1**. Predicted and observed pharmacokinetic parameters are summarized in **Table S1d of Supplement S1**.

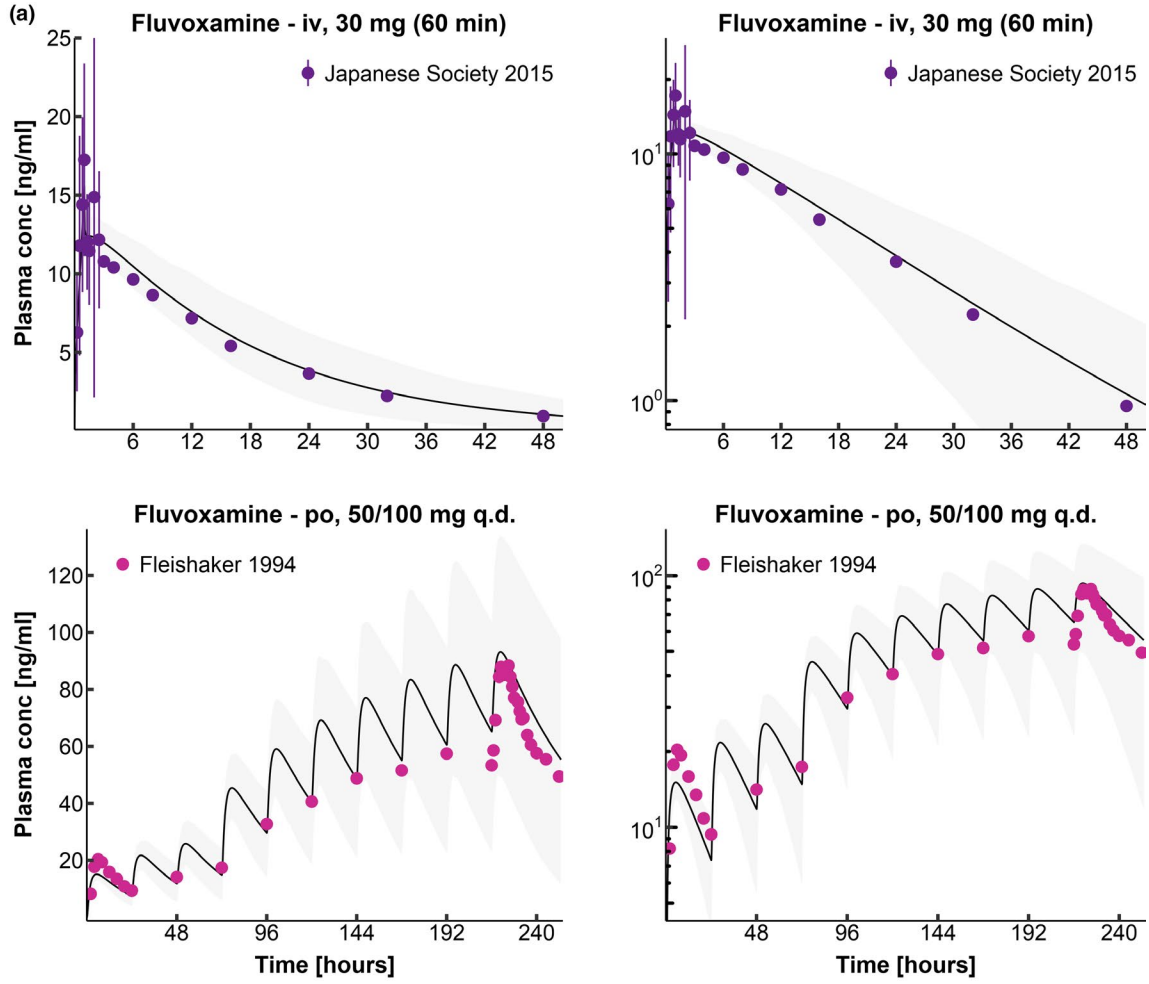
(a)
Fluvoxamine - iv, 30 mg (60 min)
Japanese Society 2015
Plasma conc [ng/ml]
Fluvoxamine - iv, 30 mg (60 min)
Japanese Society 2015
Fluvoxamine - po, 50/100 mg q.d.
Fleishaker 1994
Plasma conc [ng/ml]
Time [hours]
Fluvoxamine - po, 50/100 mg q.d.
Fleishaker 1994
Time [hours]

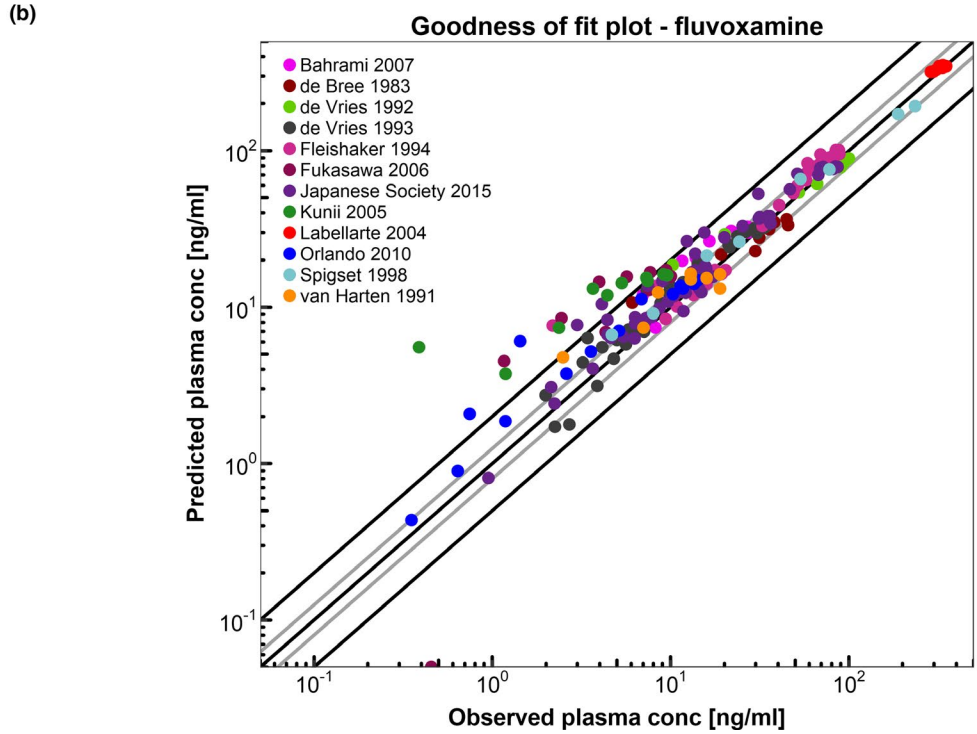
(b)
Goodness of fit plot - fluvoxamine
Bahrami 2007
de Bree 1983
de Vries 1992
de Vries 1993
Fleishaker 1994
Fukasawa 2006
Japanese Society 2015
Kunii 2005
Labellarte 2004
Orlando 2010
Spigset 1998
van Harten 1991
Predicted plasma conc [ng/ml]
Observed plasma conc [ng/ml]

caffeine,[15] rifampicin,[13] and midazolam[13] have been expanded and coupled for mutual validation of the DDI performance of these five models. The evaluation of the single models and of the network was accomplished by prediction of multiple clinical DDI studies, demonstrating their performance with different victim or perpetrator drugs. **Figure 1** shows the successfully developed CYP1A2 PBPK DDI network, with caffeine and theophylline as sensitive substrates, fluvoxamine as a strong inhibitor, and rifampicin and smoking as moderate inducers (owing to the lack of strong CYP1A2 inducers). The evaluation of the final fluvoxamine PBPK model, including the fluvoxamine fraction metabolized via CYP2D6, was supported by a *post hoc* population pharmacokinetic (PopPK) analysis to confirm the PBPK results concerning the impact of CYP2D6 poor metabolism and smoking on the metabolism of fluvoxamine. The supplementary document (**Supplement S1**) to this paper was devised as comprehensive documentation and reference guide and provides detailed information on the single models and modeled DDI studies, including all model parameters, plots, and quantitative assessments of model performance.

## METHODS

### Software

PBPK modeling was performed with PK-Sim and MoBi modeling software version 7.3.0 (part of the Open Systems Pharmacology Suite,[16] www.open-systems-pharmacology.org). Parameter optimization was accomplished using the Monte Carlo algorithm implemented in PK-Sim. Sensitivity analysis was performed within PK-Sim. PopPK analysis was performed with NONMEM version 7.3 (ICON Development Solutions, Ellicott City, MD). Digitization of published plasma concentration-time profiles was accomplished using GetData Graph Digitizer version 2.26.0.20 (S. Fedorov). PK parameter analysis was performed with MATLAB version R2013b (The MathWorks, Natick, MA). Graphics were compiled with R version 3.5.1 (The R Foundation for Statistical Computing, Vienna, Austria) and RStudio version 1.1.453 (RStudio, Boston, MA). SAS version 9.4 (SAS Institute, Cary, NC) was used for statistical analysis and graphics of the PopPK analysis.

### PBPK model building

Fluvoxamine and theophylline PBPK model building was started with an extensive literature search to collect physicochemical parameters, information on absorption, distribution, metabolism, and excretion processes and clinical studies of i.v. and p.o. administration of fluvoxamine and theophylline in single-dose and multiple-dose regimens.

The PBPK models were built based on healthy individuals, using the reported mean values for age, weight, height, and genetic background for each study protocol. If no information on these parameters could be found, a healthy male European individual, 30 years of age, with a body weight of 73 kg and a height of 176 cm was used.

To model the specific metabolic clearance, relevant CYP enzymes were implemented in accordance with literature, using the PK-Sim expression database reverse transcription-polymerase chain reaction profiles[17] to define their relative expression in the different organs of the body. For more details see **Table S6 in Supplement S1**. Glomerular filtration and enterohepatic cycling were enabled, as they are active under physiological conditions.

To build the data sets for PBPK modeling, the reported observed plasma concentration-time profiles were digitized and divided into "training data set" and "test data set." Model parameters that could not be informed from experimental reports were optimized by simultaneously fitting the model to all measured plasma concentration-time profiles assigned to the training data set. To limit the parameters to be optimized during model building, the minimal number of processes necessary was implemented into the model. Model evaluation was carried out based on the clinical data of the test data set. Descriptive (training data set) and predictive (test data set) performance of the model for all published clinical studies is transparently presented in **Supplement S1**.

### PBPK model evaluation

Model performance was evaluated with different methods. The predicted population plasma concentration-time profiles were compared with the plasma concentration-time profiles observed in the clinical studies. Furthermore, predicted plasma concentration values of all studies were compared with the observed plasma concentrations in goodness-of-fit plots. In addition, the performance was evaluated by comparison of predicted to observed area under the plasma curve (AUC) and peak plasma concentration ($C_{max}$) values. As quantitative measures of the descriptive and predictive performance of the models, the mean relative deviation (MRD) according to Edginton *et al.*[18] and the geometric mean fold error (GMFE) were calculated. MRD was calculated for all observed plasma concentrations according to Eq. 1.

$$\mathrm{MRD} = 10^{x}; x = \sqrt{\frac{\sum_{i=1}^{N} (\log_{10} c_{\mathrm{obs}} - \log_{10} c_{\mathrm{pred}})^2}{N}} \qquad (1)$$

with $\log_{10} c_{obs}$ = logarithm of the observed plasma concentration, $\log_{10} c_{pred}$ = logarithm of the predicted plasma concentration, and $N$ = number of observed values. An MRD value ≤ 2 characterizes an adequate prediction.

**Figure 3** Theophylline plasma concentrations. (**a**) Population predictions of selected theophylline plasma concentration-time profiles compared with observed data in linear (left panel) and semilogarithmic plots (right panel). The upper panel shows i.v. application, the lower panel p.o. administration of theophylline. Observed data are shown as dots ± SD.[36,37] Population simulation arithmetic means are shown as lines, and the shaded areas illustrate the 68% population prediction intervals. (**b**) Predicted compared with observed theophylline plasma concentration values of all clinical studies. Line of identity and 0.5-fold to 2.0-fold acceptance limits are shown as black lines. The 0.8-fold to 1.25-fold limits are shown as grey lines. Details on dosing regimens and study populations are listed in **Table S2a of Supplement S1**. Predicted and observed pharmacokinetic parameters are summarized in **Table S2d of Supplement S1**.

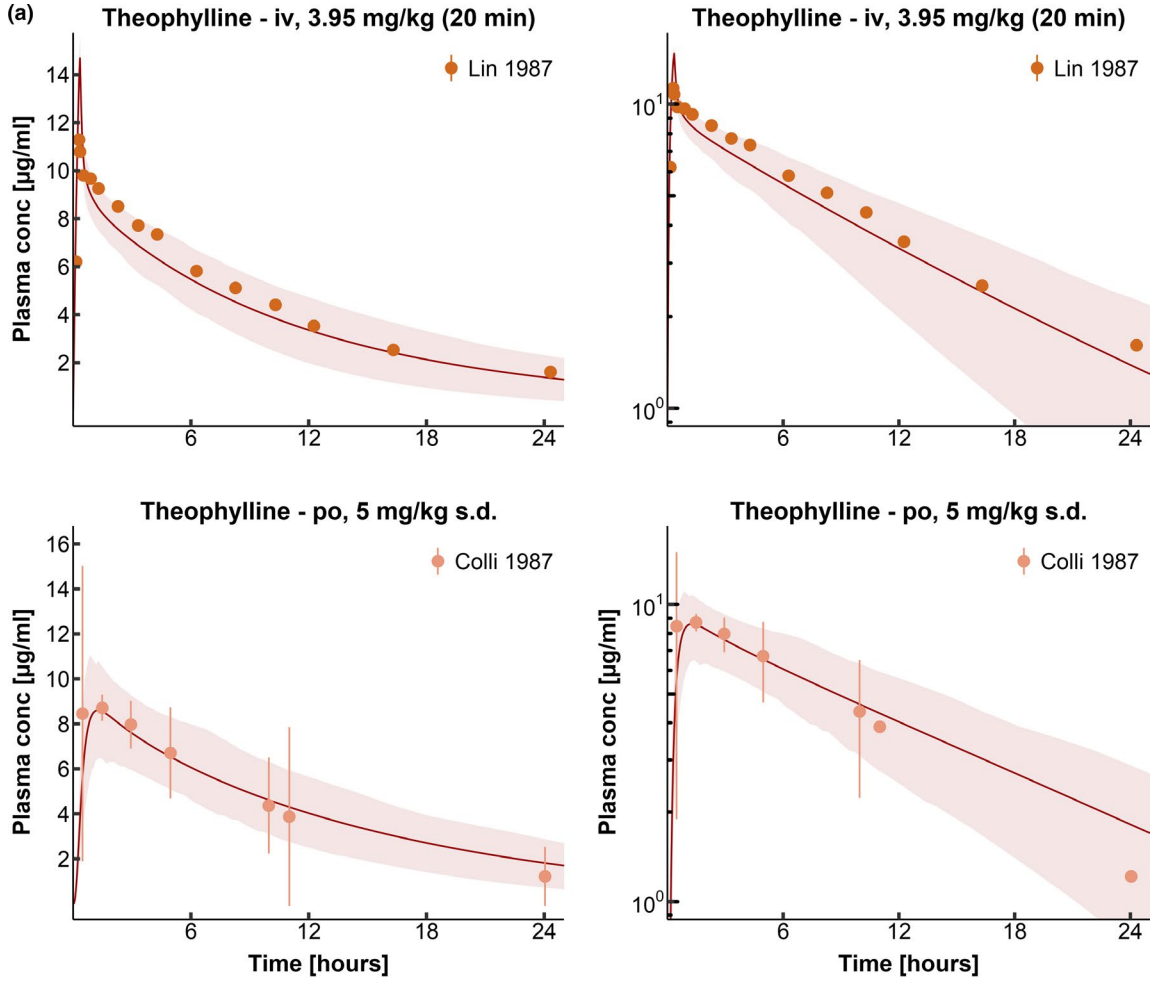
(a)
Theophylline - iv, 3.95 mg/kg (20 min)
Lin 1987
Plasma conc [µg/ml]
Theophylline - po, 5 mg/kg s.d.
Colli 1987
Time [hours]

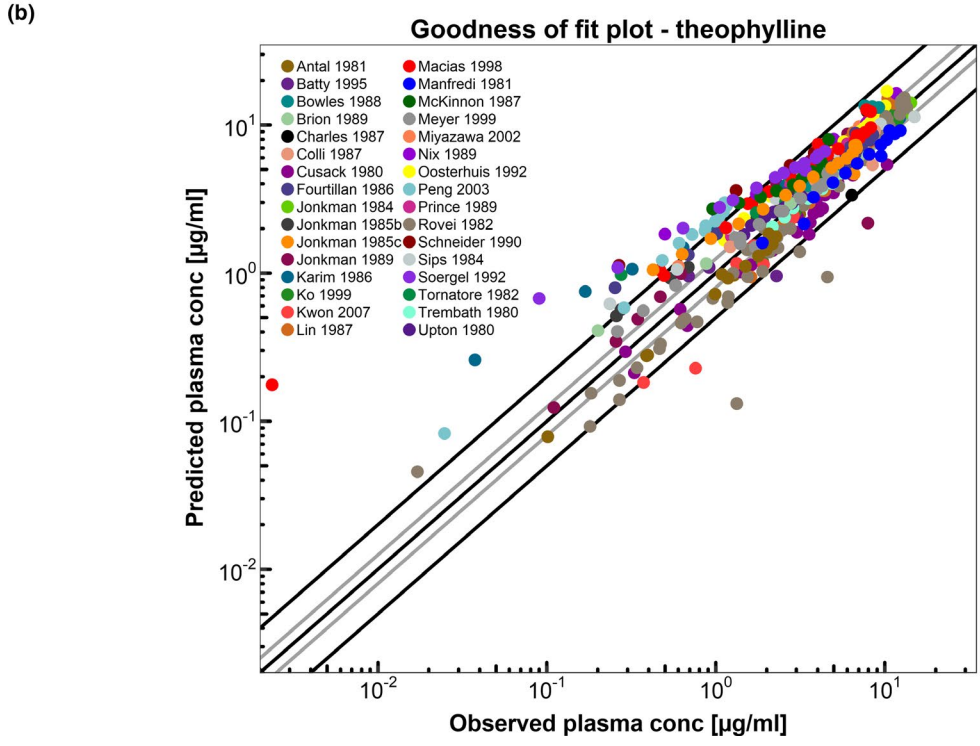
(b)
Goodness of fit plot - theophylline
Antal 1981
Batty 1995
Bowles 1988
Brion 1989
Charles 1987
Colli 1987
Cusack 1980
Fourtillan 1986
Jonkman 1984
Jonkman 1985b
Jonkman 1985c
Jonkman 1989
Karim 1986
Ko 1999
Kwon 2007
Lin 1987
Macias 1998
Manfredi 1981
McKinnon 1987
Meyer 1999
Miyazawa 2002
Nix 1989
Oosterhuis 1992
Peng 2003
Prince 1989
Rovei 1982
Schneider 1990
Sips 1984
Soergel 1992
Tornatore 1982
Trembath 1980
Upton 1980
Predicted plasma conc [µg/ml]
Observed plasma conc [µg/ml]

The GMFE was calculated for all observed AUC and $C_{max}$ values according to Eq. 2.

$$GMFE = 10^{\left(\Sigma\left|\log_{10}\left(\frac{\text{pred PK parameter}}{\text{obs PK parameter}}\right)\right|\right)/n} \quad (2)$$

with pred PK parameter = predicted AUC or $C_{max}$ value, obs PK parameter = observed AUC or $C_{max}$ value, and $n$ = number of studies. A GMFE value below two characterizes an adequate prediction.

### PopPK model building and evaluation

Fluvoxamine PBPK model evaluation was supported by a *post hoc* PopPK analysis to quantify the effect of CYP2D6 poor metabolism and the impact of smoking on fluvoxamine clearance and to compare the results to the effect sizes predicted by the PBPK model.

PopPK analysis, model evaluation, and simulation were performed using nonlinear mixed-effects modeling techniques implemented in NONMEM. A full description of the PopPK methodology is available in **Supplement S1**.

### DDI network building

In addition to the evaluation methods described above, a CYP1A2 DDI network was built to evaluate the DDI performance of the developed models (**Figure 1**). Fluvoxamine was used as a CYP1A2 and CYP3A4 inhibitor theophylline and caffeine as CYP1A2 victim drugs, rifampicin as CYP1A2 and CYP2E1 inducer, and midazolam as a CYP3A4 victim drug. Mathematical implementation of the drug interaction processes in general is specified in **Supplement S1**. All induction and inhibition processes were modeled using interaction parameter values from *in vitro* experimental reports without further adjustment or fitting.

### DDI network evaluation

All predicted DDI simulations were evaluated by comparison of predicted vs. observed victim drug plasma concentration-time profiles alone and during coadministration, DDI AUC ratios (Eq. 3), and DDI $C_{max}$ ratios (Eq. 4).

$$\text{DDI AUC ratio} = \frac{AUC_{\text{victim drug during coadministration}}}{AUC_{\text{victim drug alone}}} \quad (3)$$

$$\text{DDI } C_{max}\text{ratio} = \frac{C_{max_{\text{victim drug during coadministration}}}}{C_{max_{\text{victim drug alone}}}} \quad (4)$$

As a quantitative measure of the prediction accuracy for each DDI interaction, GMFEs of the predicted DDI AUC ratios and DDI $C_{max}$ ratios were calculated according to Eq. 2.

### Sensitivity analysis

Sensitivity of the final PBPK models to single parameters (local sensitivity analysis) was calculated, measured as relative changes of the AUC of one dosing interval in steady-state conditions for simulations of the highest recommended doses for fluvoxamine (300 mg once daily) and theophylline (500 mg once daily), respectively.

Parameters were included into the analysis if they have been optimized (**Table S1b or S2b in Supplement S1**), if they might have a strong influence due to calculation methods used in the model (fraction unbound) or if they had significant impact in former models (solubility, blood/plasma ratio, and glomerular filtration rate fraction).

Sensitivity to a parameter is calculated as the ratio of the relative change of the simulated AUC to the relative variation of the parameter around the value used in the final model according to Eq. 5.

$$S = \frac{\Delta AUC}{AUC} * \frac{p}{\Delta p} \quad (5)$$

with $S$ = sensitivity of the AUC to the examined model parameter, $\Delta$AUC = change of the AUC, AUC = simulated AUC with the original parameter value, $\Delta p$ = change of the examined model parameter value, and $p$ = original model parameter value. A sensitivity value of + 1.0 signifies that a 10% increase of the examined parameter causes a 10% increase of the simulated AUC.

### Virtual population characteristics

To predict the variability of the simulated plasma concentration-time profiles, virtual populations of 100 individuals were generated, containing European, Asian, or Japanese individuals. The percentage of male and female individuals and the age and weight ranges were set corresponding with the reported demographics. If not specified, virtual populations containing 50 male and 50 female individuals 20–50 years of age were used, without specific body weight or height restriction as implemented in the software. For details on study populations see **Tables S1a, S2a, S7a, S8a, S9a, and S10a in Supplement S1**. In the generated virtual populations, corresponding organ volumes, tissue compositions, blood flow rates, etc. were varied by an implemented algorithm within the limits of the International Commission on Radiological Protection,[19,20] Tanaka and Kawamura,[21] or Japanese[22] databases. In addition, the reference concentrations of the implemented CYP enzymes were set to be distributed with the default variabilities for their expression available in PK-Sim. **Table S6 in Supplement S1** summarized the implemented enzymes with their reference concentrations and variabilities.

With these populations, simulations were generated and compared with observed data. As the observed data were

**Figure 4** Plasma concentration-time profiles of the drug–drug interaction (DDI) network. Population predictions of selected plasma concentration-time profiles compared with observed data for the fluvoxamine-theophylline, rifampicin-theophylline, fluvoxamine-caffeine, and fluvoxamine-midazolam DDIs in linear (left panel) and semilogarithmic plots (right panel). Observed data are shown as dots ± SD.[38-41] Population simulation arithmetic means are shown as lines, and the shaded areas illustrate the 68% population prediction intervals. Details on dosing regimens and study populations are listed in **Tables S7a, S8a, S9a, and S10a of Supplement S1**. Predicted and observed pharmacokinetic parameters are summarized in **Tables S7b, S8b, S9b, and S10b of Supplement S1**.

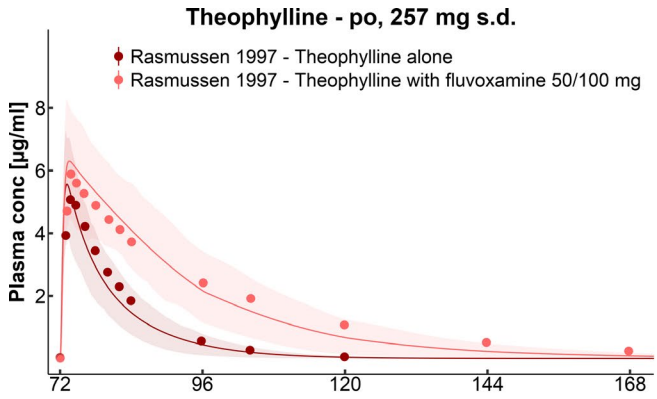
Theophylline - po, 257 mg s.d.
Rasmussen 1997 - Theophylline alone
Rasmussen 1997 - Theophylline with fluvoxamine 50/100 mg
Plasma conc [µg/ml]
2
4
6
8
72
96
120
144
168

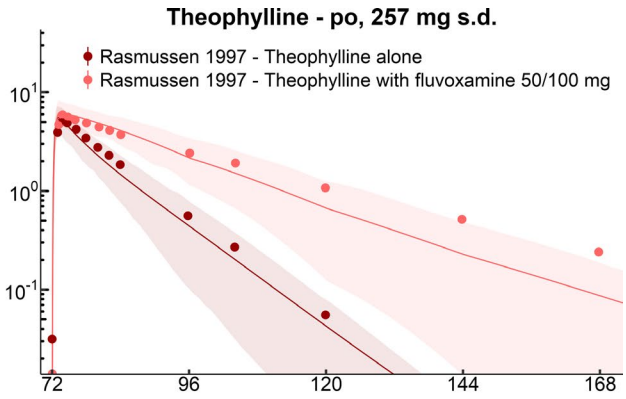
Theophylline - po, 257 mg s.d.
Rasmussen 1997 - Theophylline alone
Rasmussen 1997 - Theophylline with fluvoxamine 50/100 mg
$10^{1}$
$10^{0}$
$10^{-1}$
72
96
120
144
168

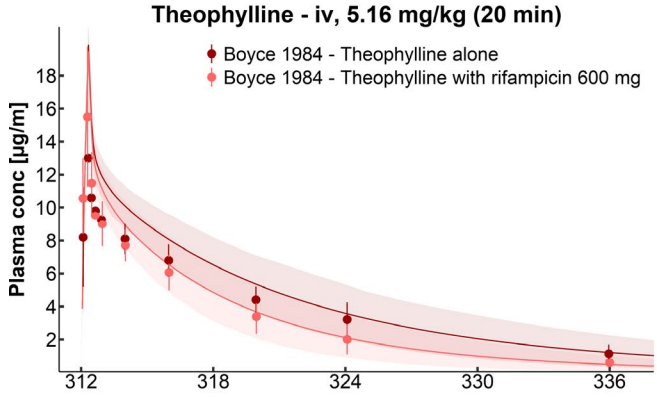
Theophylline - iv, 5.16 mg/kg (20 min)
Boyce 1984 - Theophylline alone
Boyce 1984 - Theophylline with rifampicin 600 mg
Plasma conc [µg/ml]
2
4
6
8
10
12
14
16
18
312
318
324
330
336

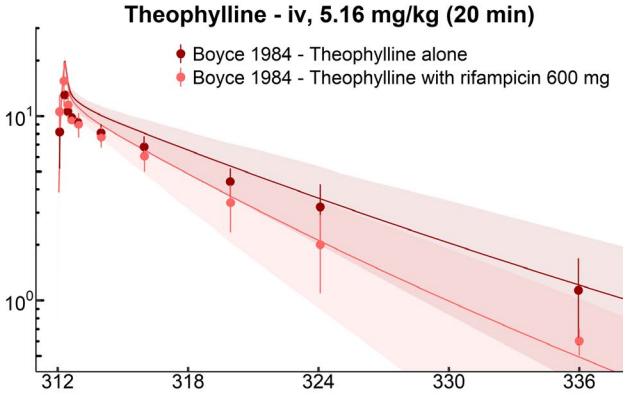
Theophylline - iv, 5.16 mg/kg (20 min)
Boyce 1984 - Theophylline alone
Boyce 1984 - Theophylline with rifampicin 600 mg
$10^{1}$
$10^{0}$
312
318
324
330
336

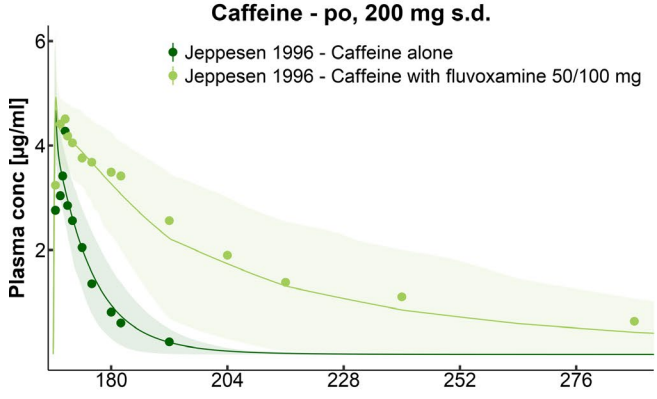
Caffeine - po, 200 mg s.d.
Jeppesen 1996 - Caffeine alone
Jeppesen 1996 - Caffeine with fluvoxamine 50/100 mg
Plasma conc [µg/ml]
2
4
6
180
204
228
252
276

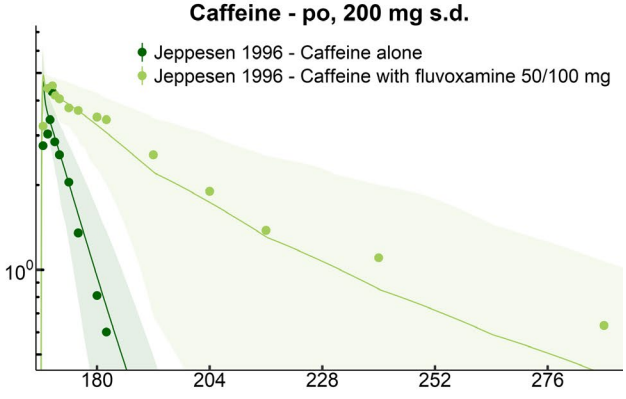
Caffeine - po, 200 mg s.d.
Jeppesen 1996 - Caffeine alone
Jeppesen 1996 - Caffeine with fluvoxamine 50/100 mg
$10^{0}$
180
204
228
252
276

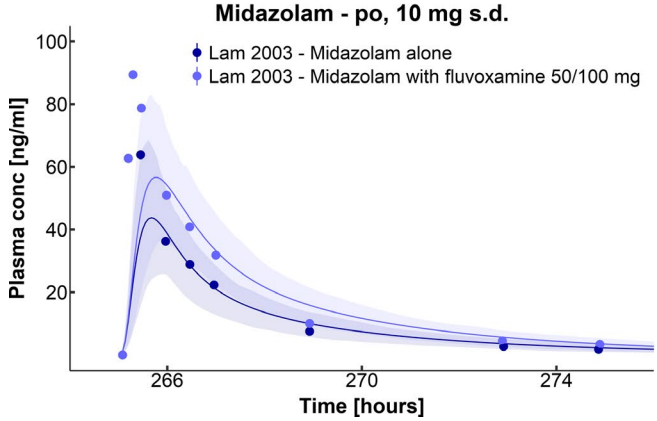
Midazolam - po, 10 mg s.d.
Lam 2003 - Midazolam alone
Lam 2003 - Midazolam with fluvoxamine 50/100 mg
Plasma conc [ng/ml]
20
40
60
80
100
266
270
274
Time [hours]

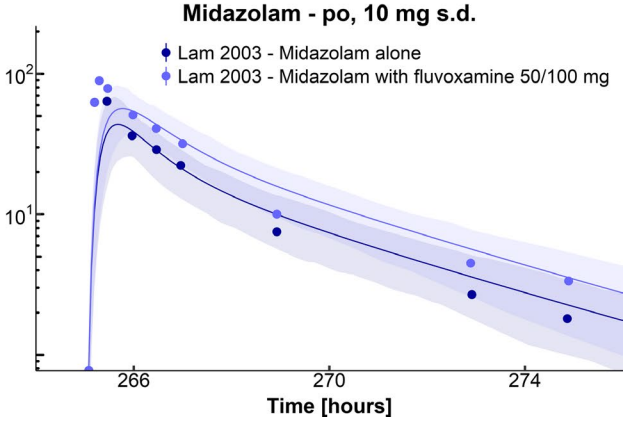
Midazolam - po, 10 mg s.d.
Lam 2003 - Midazolam alone
Lam 2003 - Midazolam with fluvoxamine 50/100 mg
$10^{2}$
$10^{1}$
266
270
274
Time [hours]

reported in terms of arithmetic means and SDs, simulated 68% population prediction intervals were plotted that correspond to the range span of ± 1 SD around the mean assuming normal distribution.

## RESULTS

### PBPK model building and evaluation

The final PBPK models of fluvoxamine and theophylline precisely describe and predict the plasma concentration-time profiles following i.v. and p.o. administration for a large range of administered doses.

Plots of population predicted compared with observed plasma concentration-time profiles of all studies obtained from literature are shown in linear as well as in semilogarithmic plots in **Figure 2a** (selected fluvoxamine studies), **Figure 3a** (selected theophylline studies), and **Figures S1a, S1b, S2a, and S2b of Supplement S1** (all studies). Goodness-of-fit plots are presented in **Figure 2b** (fluvoxamine), **Figure 3b** (theophylline), and **Figures S1c and S2c of Supplement S1**. MRD values of all studies are listed in **Tables S1c and S2c of Supplement S1**.

Predicted compared with observed AUC and $C_{max}$ values of all studies with calculated GMFEs are listed in **Tables S1d and S2d of Supplement S1**. Plots showing the correlation of predicted to observed AUC and $C_{max}$ values of all studies are presented in **Figures S1f and S2d of Supplement S1**.

For fluvoxamine PBPK model development, 26 different clinical studies with PK blood sampling were used, with 9 studies assigned to the training data set (**Table S1a in Supplement S1**). The fluvoxamine PBPK model applies metabolism by CYP1A2, CYP2D6, and glomerular filtration.

To distinguish between fluvoxamine metabolism in CYP2D6 extensive metabolizers (EMs) and poor metabolizers (PMs), the CYP2D6 catalytic rate constant ($k_{cat}$) of PMs was set to zero. This assumption was made because CYP2D6 PMs were characterized by absent CYP2D6 enzymatic activity,[23] which results in a predicted 1.5-fold increase of the fluvoxamine AUC in CYP2D6 PMs compared with CYP2D6 EMs (observed: 1.3-fold increase[24]). Population predictions of fluvoxamine plasma concentration-time profiles compared with observed data for CYP2D6 EMs and PMs are shown in **Figure S1d of Supplement S1**.

Furthermore, the final model is able to describe the influence of smoking on the PK of fluvoxamine. Smoking is the strongest known inducer of CYP1A2 and results in higher metabolism of CYP1A2 substrates.[1] As no detailed information on the frequency, duration, and amount of smoking was available from literature, the induction of CYP1A2 was implemented as a static 1.38-fold increase in enzyme activity. This factor was optimized based on the study of Spigset *et al.*,[25] resulting in a 39% reduction of the fluvoxamine AUC in smokers (observed: 31% reduction). Population predictions of fluvoxamine plasma concentration-time profiles compared with observed data for nonsmokers and smokers are shown in **Figure S1e of Supplement S1**. Drug-dependent parameters of the final fluvoxamine model are listed in **Table S1b of Supplement S1**. System-dependent parameters are given in **Table S6 of Supplement S1**.

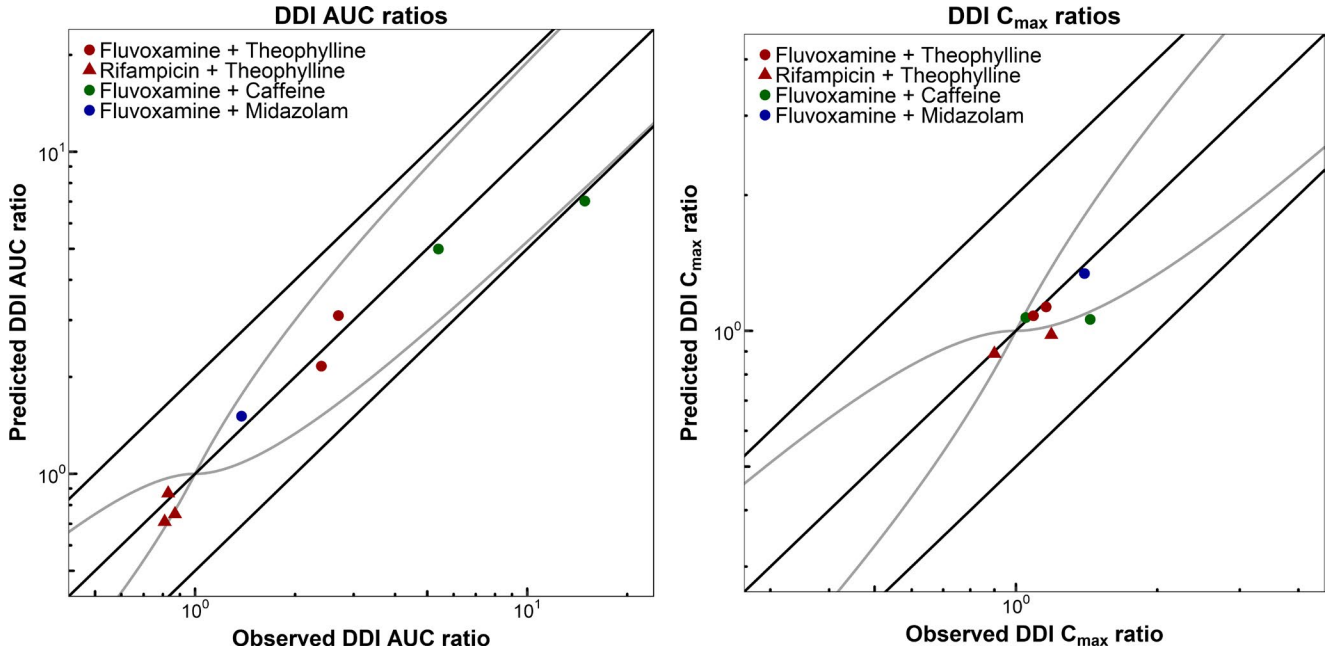


**Figure 5** Correlation of predicted to observed drug–drug interaction (DDI) area under the curve (AUC) ratios, and DDI peak plasma concentration ($C_{max}$) ratios. The left panel illustrates the predicted compared with observed DDI AUC ratios, the right panel illustrates the predicted compared with observed DDI $C_{max}$ ratios of the fluvoxamine-theophylline, rifampicin-theophylline, fluvoxamine-caffeine, and fluvoxamine-midazolam DDIs. Fluvoxamine interaction studies are shown as dots and rifampicin interaction studies are shown as triangles. The colors represent the different victim drugs. The line of identity and the 0.5-fold to 2.0-fold acceptance limits are shown as straight black lines. The curved grey lines are the prediction acceptance limits proposed by Guest *et al.*[42] Study references, dosing regimens, and values of predicted and observed DDI AUC ratios and DDI $C_{max}$ ratios are listed in **Table 1**.

Sensitivity analysis of a simulation of 300 mg fluvoxamine p.o. once daily with a sensitivity threshold of 0.5 reveals that the fluvoxamine model is sensitive to the values of lipophilicity (optimized), CYP2D6 catalytic rate constant (optimized), CYP2D6 Michaelis-Menten constant (literature value), and fraction unbound (literature value; see **Figure S1g of Supplement S1**).

For theophylline PBPK model development, 40 different clinical studies with PK blood sampling and additional fraction excreted unchanged to urine measurements and CYP1A2 fraction metabolized information were used, with 13 clinical studies assigned to the training data set (**Table S2a in Supplement S1**). The theophylline PBPK model applies metabolism by CYP1A2, CYP2E1, and glomerular filtration with reabsorption in the renal tubulus.

In the model, CYP1A2 metabolizes theophylline with high affinity but low capacity, whereas CYP2E1 metabolizes theophylline with low affinity and high capacity, as described in the literature,[26] resulting in a good prediction of the observed concentration dependency of theophylline metabolism. About 95% of an administered theophylline dose are excreted with the urine but only 14–17% as unchanged drug.[27,28] Due to the lack of valid *in vitro* data on renal tubular reabsorption transporters for theophylline, the glomerular filtration rate fraction was optimized to a value of 0.22 to describe the fraction of theophylline excreted unchanged to urine. Drug-dependent parameters of the final theophylline model are listed in **Table S2b of Supplement S1**. System-dependent parameters are given in **Table S6 of Supplement S1**.

Sensitivity analysis of a simulation of 500 mg theophylline p.o. once daily with a sensitivity threshold of 0.5 reveals that the theophylline model is sensitive to the values of fraction unbound (literature value), CYP1A2 catalytic rate constant (optimized), and CYP1A2 Michaelis-Menten constant (literature value; see **Figure S2e of Supplement S1**).

## DDI network modeling

For the CYP1A2 DDI network modeling, eight different clinical DDI studies were available, consisting of two studies of fluvoxamine with theophylline, three studies

**Table 1 DDI AUC ratios, DDI $C_{max}$ ratios, and GMFE values of DDI studies**

| Perpetrator drug | Victim drug | Observed DDI AUC ratio | Predicted DDI AUC ratio | Pred/Obs DDI AUC ratio | Observed DDI $C_{max}$ ratio | Predicted DDI $C_{max}$ ratio | Pred/Obs DD $C_{max}$ ratio | Reference |
|---|---|---|---|---|---|---|---|---|
| *Fluvoxamine* | *Theophylline* | | | | | | | |
| 50 mg p.o., q.d./b.i.d. | 3.21 mg/kg p.o., s.d. | 2.40 | 2.16 | 0.90 | 1.09 | 1.08 | 0.99 | Orlando 2006[43] |
| 50/100 mg p.o., q.d. | 257 mg p.o., s.d. | 2.70 | 3.10 | 1.15 | 1.16 | 1.13 | 0.97 | Rasmussen 1997[38] |
| | | | GMFE (range) | 1.13 (1.11–1.15) | | | 1.02 (1.01–1.03) | |
| | | Pred/Obs within twofold | | 2/2 | | | 2/2 | |
| *Rifampicin* | *Theophylline* | | | | | | | |
| 600 mg p.o., q.d. | 3.95 mg/kg i.v. (30 minutes) | 0.83 | 0.87 | 1.05 | | 0.98 | | Powell-Jackson 1985[44] |
| 600 mg p.o., q.d. | 5.19 mg/kg i.v. (20 minutes) | 0.81 | 0.71 | 0.89 | 1.19 | 0.98 | 0.82 | Boyce 1984[39] |
| 600 mg p.o., q.d. | 355.5 mg p.o., s.d. | 0.87 | 0.75 | 0.87 | 0.90 | 0.89 | 0.99 | Powell-Jackson 1985[44] |
| | | | GMFE (range) | 1.12 (1.05–1.16) | | | 1.11 (1.01–1.21) | |
| | | Pred/Obs within twofold | | 3/3 | | | 2/2 | |
| *Fluvoxamine* | *Caffeine* | | | | | | | |
| 50/100 mg p.o., q.d. | 200 mg p.o., s.d. | 5.40 | 4.99 | 0.92 | 1.06 | 1.07 | 1.01 | Jeppesen 1996[40] |
| 100 mg p.o., b.i.d | 250 mg p.o., s.d. | 14.90 | 7.03 | 0.47 | 1.44 | 1.06 | 0.74 | Culm-Merdek 2005[45] |
| | | | GMFE (range) | 1.51 (1.08–2.12) | | | 1.17 (1.01–1.36) | |
| | | Pred/Obs within twofold | | 1/2 | | | 2/2 | |
| *Fluvoxamine* | *Midazolam* | | | | | | | |
| 50 mg p.o., b.i.d. | 10 mg p.o., s.d. | 1.38 | 1.51 | 1.09 | 1.40 | 1.34 | 0.95 | Lam 2003[41] |
| | | | GMFE | 1.09 | | | 1.04 | |
| | | Pred/Obs within twofold | | 1/1 | | | 1/1 | |

AUC, area under the plasma concentration-time curve; $C_{max}$, peak plasma concentration; DDI, drug-drug interaction; GMFE, geometric mean fold error; Pred/Obs, predicted/observed; -, no data available.

of rifampicin with theophylline, two studies of fluvoxamine with caffeine, and one study of fluvoxamine with midazolam. The victim drug plasma concentration-time profiles of these studies, before and during perpetrator treatment, were predicted and compared with observed data. **Tables S7a, S8a, S9a, and S10a of Supplement S1** list the administration protocols and study population details of the clinical DDI studies. The parameters to model the CYP1A2, CYP2E1, and CYP3A4 induction and inhibition processes are described in **Supplement S1**. Population predictions of plasma concentration-time profiles of the different victim drugs before and during coadministration are presented in linear as well as semilogarithmic plots in **Figure 4** (selected studies) and **Figures S7a, S8a, S9a, and S10a of Supplement S1** (all studies). All victim drug plasma concentration-time profiles before and during coadministration with fluvoxamine or rifampicin are well-predicted over the full range of reported administration protocols.

**Figure 5** shows the correlation of predicted to observed DDI AUC ratios and DDI $C_{max}$ ratios of the modeled DDI studies as a visualization of the performance of the entire network. **Table 1** lists the corresponding DDI AUC ratio and DDI $C_{max}$ ratio values shown in **Figure 5**, with calculated GMFE values for each perpetrator–victim drug combination, demonstrating the good performance of the developed models when applied for DDI prediction.

### PopPK modeling of fluvoxamine

The PK of fluvoxamine were best described by a one-compartment model with zero-order absorption with a lag time and linear elimination from the central compartment. As shown in **Table S11 of Supplement S1**, parameter estimates were precise. Goodness-of-fit plots (**Figure S11a in Supplement S1**) and visual predictive checks (**Figure S11b in Supplement S1**) demonstrate the good descriptive performance of the model.

The impact of CYP2D6 phenotype on total clearance of fluvoxamine was best described as a categorical covariate. Volunteers who are CYP2D6 PMs show a 22% lower total clearance of fluvoxamine compared with EMs. Furthermore, fluvoxamine clearance was found to be 28% higher in smokers compared with nonsmokers.

## DISCUSSION

The developed PBPK models of fluvoxamine and theophylline reliably describe and predict plasma concentration-time profiles over the full range of published doses and administration protocols. Their good descriptive and predictive performance has been demonstrated by comparison of predicted to observed plasma concentration-time profiles, AUC and $C_{max}$ values, calculation of MRDs and GMFEs, as well as with the prediction of different DDIs. Although the populations used for model predictions were carefully generated according to the reported study demographics, CYP1A2 and CYP2D6 show high interindividual variability, and information on smoking status and CYP2D6 phenotype were lacking in most of the study reports. This could explain why a small percentage of the fluvoxamine and theophylline studies cannot be accurately predicted using the same $k_{cat}$ values for all studies.

There are two previously published PBPK models of fluvoxamine: a minimal PBPK model (three compartments)[29] and a model built on the basis of few clinical studies (four studies).[30] For theophylline, one PBPK model has been previously reported, developed to predict the disposition of theophylline during pregnancy.[31] All three models have not been challenged by prediction of DDIs. The whole-body PBPK models presented in this study have been built using a multitude of clinical studies, are transparently documented, and they have been evaluated in a DDI network.

To describe the metabolism of fluvoxamine, CYP1A2 and CYP2D6 were implemented into the PBPK model. Model building was started with the working hypothesis that CYP2D6 accounts for up to 60% of fluvoxamine metabolism.[32] However, our PBPK analysis suggested a higher fraction of fluvoxamine metabolized by CYP1A2 than by CYP2D6. This result was supported by the finding that fluvoxamine total apparent clearance (CL/F) in CYP2D6 PMs (no CYP2D6 activity) was only 25% lower than in CYP2D6 EMs.[32] (Taking into account that CYP2D6 is also expressed in the intestine, CYP2D6 PMs might show a higher bioavailability of fluvoxamine, reducing CL/F, and thereby further reducing the impact of CYP2D6 poor metabolism on fluvoxamine clearance.)

To confirm this relatively small impact of CYP2D6 poor metabolism on fluvoxamine PK, a PopPK analysis of fluvoxamine was conducted. The reduction of fluvoxamine CL/F in CYP2D6 PMs compared with EMs was quantified at 22%. This is the first reported compartmental analysis of fluvoxamine, which is in very good agreement with the noncompartmental result for reduction of CL/F in CYP2D6 PMs of 25%.[32]

Simulation of fluvoxamine fraction metabolized using the final PBPK model and a single dose of 50 mg predicts fractions metabolized of 20% by CYP2D6 and of 71% by CYP1A2, which is very close to the PopPK analysis result. Neither fraction metabolized information nor the CYP2D6 PM fluvoxamine plasma profiles were used during the final PBPK model parameter optimization. Fitting the catalytic rate constants of CYP2D6 and CYP1A2 and, therefore, the contribution of both enzymes to fluvoxamine metabolism to get a good description of the nonlinear PK of fluvoxamine for the different doses administered already resulted in a model that accurately describes the fractions metabolized.

The inducing effect of smoking on the metabolism of fluvoxamine is also well-described by the PBPK model, with AUC ratios smoking/nonsmoking of 0.61 predicted and 0.69 observed. The fluvoxamine PopPK analysis gives a 28% higher CL/F of fluvoxamine in smokers compared with nonsmokers. The small overprediction of the fluvoxamine $C_{max}$ in smokers could be attributed to gastrointestinal effects of smoking that reduce the absorption of fluvoxamine but were not accounted for in the model. However, due to a lack of more detailed information on the frequency, duration, and amount of smoking, the induction of CYP1A2 could only be implemented as a static increase of the enzyme activity. To model this CYP induction in a mechanistic and dynamic

way, for example, to predict the return of CYP1A2 activity to baseline when smoking is stopped before a surgical intervention, as well as to validate the estimated factor on CYP1A2 enzyme activity for the smoking population, more data are needed.

The developed theophylline model can be used for prediction of plasma concentration-time profiles following i.v. administration or p.o. administration of syrup, solution, or immediate-release formulations. As the reported plasma concentration profiles of the different sustained release dosage forms strongly vary with the mechanism used for prolongation of drug release, sustained release or enteric coated theophylline formulations were not considered in the current investigation. If needed, the model can be easily extended by implementation of sustained release drug dissolution profiles.[33]

The DDIs presented in this study have been modeled using reported experimental values to inform all necessary interaction parameters. This approach is followed as an additional means of model evaluation, predicting all available reported clinical DDI studies, and comparing the observed data to model predictions. The caffeine,[15] rifampicin,[13] and midazolam[13] PBPK models applied have been evaluated and described elsewhere. The existing rifampicin model has been extended to predict the induction of CYP1A2 and CYP2E1 by rifampicin. The DDI performance of the enhanced rifampicin model has been successfully evaluated with the data of three different clinical rifampicin-theophylline DDI studies.

The presented CYP1A2 DDI network demonstrates the good performance of all models for DDI prediction over the full range of reported DDI study protocols. This has been shown by victim drug concentration-time profiles, DDI AUC ratios, DDI $C_{max}$ ratios, and corresponding GMFE values. All DDIs of fluvoxamine with the sensitive CYP1A2 victim drugs theophylline and caffeine are well predicted. The moderate inhibition of CYP3A4 by fluvoxamine was successfully implemented and evaluated by prediction of the fluvoxamine-midazolam DDI. Due to the present lack of models for CYP2C19 victim drugs, the strong inhibition of CYP2C19 by fluvoxamine could not be tested. However, fluvoxamine CYP2C19 interaction parameters are reported and can be easily implemented into the presented fluvoxamine PBPK model.

In summary, a PBPK CYP1A2 DDI network has been successfully developed. Whole-body PBPK models of fluvoxamine and theophylline have been carefully built and evaluated by DDI prediction using different kinds of perpetrator (induction, competitive inhibition, and mixed inhibition) and victim drugs (CYP1A2 and CYP3A4). Furthermore, a previously developed model of rifampicin has been expanded with parameters for CYP1A2 and CYP2E1 interaction and tested. The resulting PBPK network of fluvoxamine, theophylline, caffeine, rifampicin, and midazolam adequately predicts the observed data of all clinical DDI studies reported for combinations of these drugs and, therefore, all models are considered ready to use for DDI prediction. The newly developed models of fluvoxamine and theophylline are transparently documented and the model files, also including DDI model files, are provided as **Supplementary Material** to this paper (**Data S1-S6**) as well as in the Open Systems Pharmacology repository (www.open-systems-pharmacology.org), to extend the library of publicly available PBPK models for DDI prediction. They can be applied to help understand and characterize the DDI potential of investigational drugs, to inform the design of clinical trials, or to generate dose recommendations for comedication.

**Supporting Information.** Supplementary information accompanies this paper on the *CPT: Pharmacometrics & Systems Pharmacology* website (www.psp-journal.com).

**Supplement S1.** Model information and evaluation.
**Data S1**. Fluvoxamine model file.
**Data S2.** Theophylline model file.
**Data S3.** Fluvoxamine-theophylline DDI model file.
**Data S4.** Rifampicin-theophylline DDI model file.
**Data S5.** Fluvoxamine-caffeine DDI model file.
**Data S6.** Fluvoxamine-midazolam DDI model file.

**Funding.** This project has received funding from the European Union's Horizon 2020 Research and Innovation Programme under grant agreement No. 668353. M.S. was supported by the Robert Bosch Stiftung, Stuttgart, Germany.

**Conflict of Interest.** T.E., T.W., and S.F. are employees of Bayer AG. A.K.V. performed this work at the Saarland University. Since January 2018, she is an employee of the Federal Institute for Drugs and Medical Devices (BfArM) and declares no potential conflicts of interest with respect to the research, authorship, and/or publication of this article. No potential conflicts of interest were disclosed by the other authors.

**Author Contributions.** H.B., N.H., A.K.V., and T.L. wrote the manuscript. N.H., O.S., M.S., T.E., T.W., S.F., and T.L. designed the research. H.B., N.H., A.K.V., S.F., and T.L. performed the research.

**Disclaimer.** The views expressed in this article are the views of A.K.V. and do not necessarily reflect the views and opinions of the BfArM.

1. Zhou, S.F., Yang, L.P., Zhou, Z.W., Liu, Y.H. & Chan, E. Insights into the substrate specificity, inhibitors, regulation, and polymorphisms and the clinical impact of human cytochrome P450 1A2. *AAPS J.* **11**, 481–494 (2009).
2. Shimada, T., Yamazaki, H., Mimura, M., Inui, Y. & Guengerich, F.P. Interindividual variations in human liver cytochrome P-450 enzymes involved in the oxidation of drugs, carcinogens and toxic chemicals: studies with liver microsomes of 30 Japanese and 30 caucasians. *J. Pharmacol. Exp. Ther.* **270**, 414–423 (1994).
3. Chen, Y., Liu, L., Laille, E., Kumar, G. & Surapaneni, S. In vitro assessment of cytochrome P450 inhibition and induction potential of azacitidine. *Cancer Chemother. Pharmacol.* **65**, 995–1000 (2010).
4. Kalow, W. & Tang, B. The use of caffeine for enzyme assays: a critical appraisal. *Clin. Pharmacol. Ther.* **53**, 503–514 (1993).
5. Karjalainen, M.J., Neuvonen, P.J. & Backman, J.T. Rofecoxib is a potent, metabolism-dependent inhibitor of CYP1A2: implications for in vitro prediction of drug interactions. *Drug Metab. Dispos.* **34**, 2091–2096 (2006).
6. Lu, P. *et al.* Mechanism-based inhibition of human liver microsomal cytochrome P450 1A2 by zileuton, a 5-lipoxygenase inhibitor. *Drug Metab. Dispos.* **31**, 1352–1360 (2003).
7. Faber, M.S., Jetter, A. & Fuhr, U. Assessment of CYP1A2 activity in clinical practice: why, how, and when? *Basic Clin. Pharmacol. Toxicol.* **97**, 125–134 (2005).
8. US Food and Drug Administration. Clinical drug interaction studies - study design, data analysis, implications for dosing, and labeling recommendations. Draft Guidance for Industry <https://www.fda.gov/downloads/drugs/guidancecomplianceregulatoryinformation/guidances/ucm292362.pdf> (2017).
9. US Food and Drug Administration. Drug development and drug interactions: table of substrates, inhibitors and inducers. <https://www.fda.gov/Drugs/DevelopmentApprovalProcess/DevelopmentResources/DrugInteractionsLabeling/ucm093664.htm> (2017). Accessed October 2, 2018.

10. European Medicines Agency. Guideline on the investigation of drug interactions. <https://www.ema.europa.eu/documents/scientific-guideline/guideline-investigation-drug-interactions_en.pdf> (2015).
11. European Medicines Agency. Draft guideline on the qualification and reporting of physiologically based pharmacokinetic (PBPK) modelling and simulation. <https://www.ema.europa.eu/documents/scientific-guideline/draft-guideline-qualification-reporting-physiologically-based-pharmacokinetic-pbpk-modelling_en.pdf> (2016).
12. US Food and Drug Administration. Physiologically based pharmacokinetic analyses - format and content. Guidance for Industry. <https://www.fda.gov/downloads/Drugs/GuidanceComplianceRegulatoryInformation/Guidances/UCM531207.pdf> (2018).
13. Hanke, N. *et al.* PBPK models for CYP3A4 and P-gp DDI prediction: a modeling network of rifampicin, itraconazole, clarithromycin, midazolam, alfentanil, and digoxin. *CPT Pharmacometrics Syst. Pharmacol.* **7**, 647–659 (2018).
14. Open Systems Pharmacology (OSP). OSP repository. <https://github.com/Open-Systems-Pharmacology> (2018). Accessed October 2, 2018.
15. Open Systems Pharmacology (OSP). OSP repository: caffeine template model. <https://github.com/Open-Systems-Pharmacology/Example_Caffeine/blob/master/Caffeine.pksim5> (2018). Accessed October 2, 2018.
16. Eissing, T. *et al.* A computational systems biology software platform for multiscale modeling and simulation: integrating whole-body physiology, disease biology, and molecular reaction networks. *Front. Physiol.* **2**, 1–10 (2011).
17. Meyer, M., Schneckener, S., Ludewig, B., Kuepfer, L. & Lippert, J. Using expression data for quantification of active processes in physiologically-based pharmacokinetic modeling. *Drug Metab. Dispos.* **40**, 892–901 (2012).
18. Edginton, A.N., Schmitt, W. & Willmann, S. Development and evaluation of a generic physiologically based pharmacokinetic model for children. *Clin. Pharmacokinet.* **45**, 1013–1034 (2006).
19. Valentin, J. Basic anatomical and physiological data for use in radiological protection: reference values. A report of age- and gender-related differences in the anatomical and physiological characteristics of reference individuals. ICRP Publication 89. *Ann. ICRP* **32**, 5–265 (2002).
20. Willmann, S. *et al.* Development of a physiology-based whole-body population model for assessing the influence of individual variability on the pharmacokinetics of drugs. *J. Pharmacokinet. Pharmacodyn.* **34**, 401–431 (2007).
21. Tanaka, G. & Kawamura, H. Anatomical and physiological characteristics for Asian reference man: male and female of different ages: Tanaka model. Division of Radioecology, National Institute of Radiological Sciences. Hitachinaka 311-12 Japan. NIRS-M-115 (1996).
22. Open Systems Pharmacology Suite. Open Systems Pharmacology Suite Manual, Version 7.0.0. (2017).
23. Crews, K.R. *et al.* Clinical Pharmacogenetics Implementation Consortium guidelines for cytochrome P450 2D6 genotype and codeine therapy: 2014 update. *Clin. Pharmacol. Ther.* **95**, 376–382 (2014).
24. Spigset, O., Granberg, K., Hägg, S., Norström, A. & Dahlqvist, R. Relationship between fluvoxamine pharmacokinetics and CYP2D6/CYP2C19 phenotype polymorphisms. *Eur. J. Clin. Pharmacol.* **52**, 129–133 (1997).
25. Spigset, O., Carleborg, L., Hedenmalm, K. & Dahlqvist, R. Effect of cigarette smoking on fluvoxamine pharmacokinetics in humans. *Clin. Pharmacol. Ther.* **58**, 399–403 (1995).
26. Zhang, Z. & Kaminsky, L.S. Characterization of human cytochromes P450 involved in theophylline 8-hydroxylation. *Biochem. Pharmacol.* **50**, 205–211 (1995).
27. Macias, W.L. *et al.* Lack of effect of olanzapine on the pharmacokinetics of a single aminophylline dose in healthy men. *Pharmacotherapy* **18**, 1237–1248 (1998).
28. Rovei, V., Chanoine, F. & Strolin Benedetti, M. Pharmacokinetics of theophylline: a dose-range study. *Br. J. Clin. Pharmacol.* **14**, 769–778 (1982).
29. Iga, K. Use of three-compartment physiologically based pharmacokinetic modeling to predict hepatic blood levels of fluvoxamine relevant for drug-drug interactions. *J. Pharm. Sci.* **104**, 1478–1491 (2015).
30. Alqahtani, S. & Kaddoumi, A. Development of a physiologically based pharmacokinetic/pharmacodynamic model to predict the impact of genetic polymorphisms on the pharmacokinetics and pharmacodynamics represented by receptor/transporter occupancy of central nervous system drugs. *Clin. Pharmacokinet.* **55**, 957–969 (2016).
31. Ke, A.B. *et al.* A physiologically based pharmacokinetic model to predict disposition of CYP2D6 and CYP1A2 metabolized drugs in pregnant women. *Drug Metab. Dispos.* **41**, 801–813 (2013).
32. Spigset, O., Axelsson, S., Norström, A., Hägg, S. & Dahlqvist, R. The major fluvoxamine metabolite in urine is formed by CYP2D6. *Eur. J. Clin. Pharmacol.* **57**, 653–658 (2001).
33. Thelen, K., Coboeken, K., Willmann, S., Dressman, J.B. & Lippert, J. Evolution of a detailed physiological model to simulate the gastrointestinal transit and absorption process in humans, part II: extension to describe performance of solid dosage forms. *J. Pharm. Sci.* **101**, 1267–1280 (2012).
34. Japanese Society of Hospital Pharmacists. Pharmaceutical interview form (Article in Japanese). <https://www.abbvie.co.jp/content/dam/abbviecorp/japan/docs/if_luvox_201412.pdf> (2015). Accessed October 2, 2018.
35. Fleishaker, J. & Hulst, L. A pharmacokinetic and pharmacodynamic evaluation of the combined administration of alprazolam and fluvoxamine. *Eur. J. Clin. Pharmacol.* **46**, 35–39 (1994).
36. Lin, J.H., Chremos, A.N., Chiou, R., Yeh, K.C. & Williams, R. Comparative effect of famotidine and cimetidine on the pharmacokinetics of theophylline in normal volunteers. *Br. J. Clin. Pharmacol.* **24**, 669–672 (1987).
37. Colli, A. *et al.* Ticlopidine-theophylline interaction. *Clin. Pharmacol. Ther.* **41**, 358–362 (1987).
38. Rasmussen, B.B., Jeppesen, U., Gaist, D. & Brøsen, K. Griseofulvin and fluvoxamine interactions with the metabolism of theophylline. Ther. Drug Monit. **19**, 56–62 (1997).
39. Boyce, E.G. The effect of rifampin on theophylline pharmacokinetic parameters (following intravenous aminophylline) in normal volunteers. (1984).
40. Jeppesen, U., Loft, S., Poulsen, H.E. & Brøsen, K. A fluvoxamine-caffeine interaction study. Pharmacogenetics **6**, 213–222 (1996).
41. Lam, Y.W.F., Alfaro, C.L., Ereshefsky, L. & Miller, M. Pharmacokinetic and pharmacodynamic interactions of oral midazolam with ketoconazole, fluoxetine, fluvoxamine, and nefazodone. J. Clin. Pharmacol. **43**, 1274–1282 (2003).
42. Guest, E.J., Aarons, L., Houston, J.B., Rostami-Hodjegan, A. & Galetin, A. Critique of the two-fold measure of prediction success for ratios: application for the assessment of drug-drug interactions. Drug Metab. Dispos. **39**, 170–173 (2011).
43. Orlando, R., *et al.* Liver dysfunction markedly decreases the inhibition of cytochrome P450 1A2-mediated theophylline metabolism by fluvoxamine. Clin. Pharmacol. Ther. **79**, 489–499 (2006).
44. Powell-Jackson, P.R., Jamieson, A.P., Gray, B.J., Moxham, J. & Williams, R. Effect of rifampicin administration on theophylline pharmacokinetics in humans. Am. Rev. Respir. Dis. **131**, 939–940 (1985).
45. Culm-Merdek, K.E., von Moltke, L.L., Harmatz, J.S. & Greenblatt, D.J. Fluvoxamine impairs single-dose caffeine clearance without altering caffeine pharmacodynamics. Br. J. Clin. Pharmacol. **60**, 486–493 (2005).

**© 2019 The Authors *CPT: Pharmacometrics & Systems Pharmacology* published by Wiley Periodicals, Inc. on behalf of the American Society for Clinical Pharmacology and Therapeutics. This is an open access article under the terms of the Creative Commons Attribution-NonCommercial License, which permits use, distribution and reproduction in any medium, provided the original work is properly cited and is not used for commercial purposes.**